Kshirsagar et al. 2016. *Int. J. Vehicle Structures & Systems*, 8(2), 58-66
ISSN: 0975-3060 (Print), 0975-3540 (Online)
doi: 10.4273/ijvss.8.2.01

International Journal of Vehicle Structures & Systems
Available online at www.maftree.org/eja

Design Optimization of Rocker Bogie System and Development of Look-Up Table for Reconfigurable Wheels for a Planetary Rover

Alap Kshirsagar[a] and Anirban Guha

Dept. of Mech. Engg., Indian Institute of Technology, Mumbai, India
[a]Corresponding Author, Email: alapkshirsagar@gmail.com

ABSTRACT:

Planetary rovers offer promising alternatives for conducting in-situ experiments on other planets. Considering the huge costs of such exploration missions, it becomes necessary to design an optimal mobility system configuration to meet the mission goals. In this paper, a constrained optimization procedure is presented to obtain optimal design parameters of rocker-bogie mobility system. More recently, researchers have proposed the idea of using reconfigurable wheels, which would be able to change their shape according to the terrain, to improve rover's performance. One of the major challenges in implementation of such wheels is their control and autonomy. To avoid complex on-board calculations, the method of using look-up table for autonomously changing the wheel dimensions is proposed in this paper. For obtaining this look-up table, physics based motion dynamics simulation model is developed, incorporating the wheel-soil contact mechanics and motion dynamics of the rocker bogie mobility system. The simulated motion of rocker bogie is found to be in conformance with the ground profile. Performance metrics like slip ratio, effective ground pressure and power consumption are evaluated through the motion simulations. Finally, a lookup table for autonomous shape changing wheels is presented for certain terrain characteristics.

KEYWORDS:

Design optimization; Planetary rover; Terra mechanics, Motion dynamics; Reconfigurable wheels

CITATION:

A. Kshirsagar and A. Guha. 2016. Design Optimization of Rocker Bogie System and Development of Look-Up Table for Reconfigurable Wheels for a Planetary Rover, *Int. J. Vehicle Structures & Systems*, 8(2), 58-66. doi:10.4273/ijvss.8.2.01

1. Introduction

In this age of space technology, robotic exploration of solar system has been at the forefront of various space agencies in the world. Moon and Mars have been particularly focused because of their proximity to Earth. The idea of sending a rover to the surface of another planet is to allow earth bound scientists to access specific areas of interest without enduring the harsh environments of space [1]. The mobility system of rover enables it to carry scientific instruments to various terrestrial formations for in-situ experimentation. Different types of mobility systems have been proposed [1-4]. Currently the most successful mobility system is the rocker-bogie suspension system used by NASA for all of its Mars rovers after Sojourner. The rocker-bogie suspension mechanism, along with a differential, enables a six-wheeled vehicle to passively keep all six wheels in contact with a surface even when driving on severely uneven terrain [3].

The performance of the mobility system is affected by the design parameters such as link lengths, wheel dimensions and center of mass. Therefore it is important to obtain optimal design parameters of the rocker bogie system. The performance of rocker bogie system is measured in terms of power consumption and effective ground pressure in this paper. The constraints on design parameters are obtained by evaluating the obstacle climbing capability and load equalization condition. Experiences with spirit and opportunity, the twin Mars Exploration Rovers, showed that one of the major issues that need to be addressed in order to expand the exploration capabilities of planetary rovers is that of wheel traction. The relationships governing how much traction a wheel can produce are highly dependent on both the shape of the wheel and terrain properties. In the past, it has always been a challenge to find the right balance between designing a rover wheel with high traction capabilities and low power requirements. More recently, researchers have investigated the concept of a reconfigurable wheel which would have the ability to change its shape to adapt to the type of terrain it was on [5]. In challenging terrain environments, the wheel could configure to a size that would maximize traction. In less challenging terrain environments, the wheel could configure to a size that would minimize power. To autonomously determine the appropriate size of the wheel for a given terrain a method of using look up table which can be accessed by the on-board controller is discussed in this paper.

2. Rocker bogie design optimization

2.1. Design variables

Two sides of the rover are identical in the rocker-bogie suspension system. Thus for design optimization

purpose, single side of the rocker-bogie system is focused. The following ten parameters are used to define the dimensions of single side of the rocker-bogie system.

- Co-ordinates of points A and B: x_a, y_a, x_b, y_b
- Co-ordinates of center of mass of rover: x_g, y_g
- Radius and width of wheel: r, b
- Distances between wheel centers: x_1, x_2

The parameters are shown in Fig. 1, where 'c' is the length required for mounting the on-spot turning motors above front and back wheels, which is assumed to be almost equal to radius of the wheel r to simplify the calculations.

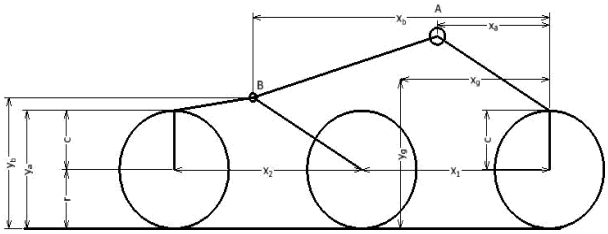

Fig. 1: Design variables for single side of rocker-bogie suspension system

2.2. Evaluation of performance metrics and design constraints

Metrics for evaluating planetary rovers provide means to assign numerical values to a system's capabilities. Numerous metrics have been proposed and used in literature such as mass, volume, system complexity, power consumption, terrain traversing capability, traction, toppling stability etc. [4]. Power consumption is an important factor as it has direct impact on the choice of electronic components and energy source. Effective ground pressure, which is a measure of average pressure exerted by wheel on ground, is important as the rover has to be designed to safely operate on soft terrain. Rovers are expected to travel over extremely uneven terrain. Thus terrain traversing capability or obstacle negotiability conditions impose constraints on design parameters. Ensuring equal load on each wheel is also important as heavier load on a single wheel might cause it to go deep in the soil.

2.2.1. Power consumption

The total power consumption of rover includes the power consumed by driving motors, steering motors and other payloads as follows,

$$P_{total} = N_w \times P_{driving} + N_s \times P_{steering} + P_{payloads} \quad (1)$$

Where N_w - No of wheels and N_s - No of independently steered wheels, Payload power consumption is independent of suspension design parameters, so it is taken as a constant. Steering motors are powered only during turning motion. Assuming the rover is moving along a straight trajectory (no turning), the total power consumption of rover is given by:

$$P_{total} = N_w \times P_{driving} + P_{payloads} \quad (2)$$

The power consumption of driving motor is given by [6]:

$$P_{driving} = \frac{\tau_{wheel} \times \omega_{wheel}}{\eta_{ampli} \times \eta_{motor} \times \eta_{gearbox}} \quad (3)$$

$$\tau_{wheel} = R_{total} \times r_{wheel} \quad (4)$$

$$\omega_{wheel} = v_{rover} / r_{wheel} \quad (5)$$

where τ_{wheel} - Driving motor torque, ω_{wheel} - Wheel angular speed, r_{wheel} - Wheel radius, v_{rover} - Forward speed of rover, η_{ampli} - Amplifier efficiency, η_{mot} - Motor efficiency and η_{gear} - Gearbox efficiency. For simplifying the calculations all efficiencies are assumed to be constant.

In Eqn. (4), the total motion resistance R_{total} is used to compute the wheel torque. It depends upon the wheel dimensions, wheel-soil interaction and terrain conditions. In most of the planetary rovers, wheels are generally metallic and their deflection under static loading is much lower than the deformation of soil/terrain. So the model of a 'Rigid wheel travelling over deformable terrain' [7] is suitable for this condition. In this model, the rolling resistance is neglected as the deformation of wheel is very small. Motion resistance of tire consists of the compaction resistance and the bulldozing resistance. Compaction resistance (R_c), represents the resistance due to terrain deformation, is using [8],

$$R_c = \frac{\left(3W/\sqrt{D}\right)^{\frac{2n+2}{2n+1}}}{(3-n)^{\frac{2n+2}{2n+1}} \times (n+1) \times b^{\frac{1}{2n+1}} \times \left(k_c/b + k_f\right)^{\frac{1}{2n+1}}} \quad (6)$$

When a substantial soil mass is displaced by a wheel, the developed bulldozing resistance (R_b) is given as [8],

$$R_b = b\left(c \times z \times k_{pc} + 0.5 \times z^2 \times \gamma \times k_{py}\right) \quad (7)$$

where z is the static sinkage of the wheel given by,

$$z = \left(\frac{3W}{(3-n)\left(k_c + bk_f\right) \times \sqrt{D}}\right)^{\frac{2n}{2n+1}} \quad (8)$$

where b - Width of wheel, k_c, k_f, n - Pressure sinkage parameters of the specific terrain, W - Normal load on wheel, D - Wheel Diameter, c - Cohesion, k_{pc}, k_{py} - Terzaghi soil factors [9] and γ - Soil density.

Apart from the resistances to motion of wheel, the rover encounters gravitational resistance (Rg) while climbing a slope, given as the projection of weight on the slope using,

$$R_g = M_{total} g_{mars} \sin(\theta) / N_w \quad (9)$$

where M_{total} - Total mass of rover, g_{mars} - Acceleration due to gravity on mars = 3.711 m/s^2 and θ - Slope angle. The mass of chassis, payload and motors will be much greater than the mass of wheels and suspension links. Therefore for simplifying the design optimization calculations, the total mass of rover can be assumed to be independent of design parameters.

2.2.2. Effective ground pressure

Effective ground pressure (EGP) is defined as the average pressure under the average wheel. The average weight on a wheel is first found by dividing the total vehicle weight on a planetary body by the number of wheels. The EGP is found by dividing the average weight by the cross sectional area of the wheel's contact patch on the ground plane [10] using,

$$Average\ weight\ per\ wheel = M_{total}\, g_{mars} / N_w \quad (10)$$

$$EGP = \frac{M_{total}\, g_{mars}}{N_w\, r_{wheel}\, b} \tag{11}$$

where M_{total} - Total mass of rover, g_{mars} - Acceleration due to gravity on mars = 3.711 m/s^2, N_w - Number of wheels, r_{wheel} - Wheel radius and b - Width of wheel.

2.2.3. Obstacle negotiability

The geometric manoeuvre of the rover is decided by the terrain geometry and the suspension parameters including the ground clearance of chassis. As shown in Fig. 2 and Fig. 3, two cases have been analysed:

Case 1: The rover is climbing over a step of height 'h', middle and front wheels have successfully climbed over the step and rear wheel has just contacted with the vertical face of barrier. Substituting the design variables in geometry relations from Fig. 2,

$$y_b - \frac{h^2 r + r^2 x_2 \sqrt{\frac{x_2^2 - h^2}{x_2^2}} - hr x_b - r x_2 x_b + h x_2 x_b \sqrt{\frac{x_2^2 - h^2}{x_2^2}}}{h^2 + r\sqrt{\frac{x_2^2 - h^2}{x_2^2}}} > 0 \tag{12}$$

Case 2: The rover is climbing over an obstacle of height 'h_2' and width 'w', middle wheel has just overcome the obstacle and landed on horizontal surface. Substituting the design variables in geometry relations from Fig. 3,

$$y_b - \frac{(h-r)(x_b - x_1)}{r} - r > 0 \tag{13}$$

$$x_2 \geq w + 2r \tag{14}$$

Also the ground clearance i.e. height of point 'A', should be greater than y_b as,

$$y_a - y_b > 0 \tag{15}$$

Thus the Eqns. (12) to (15) give the constraints on the design parameters for given obstacle dimensions and vertical step height.

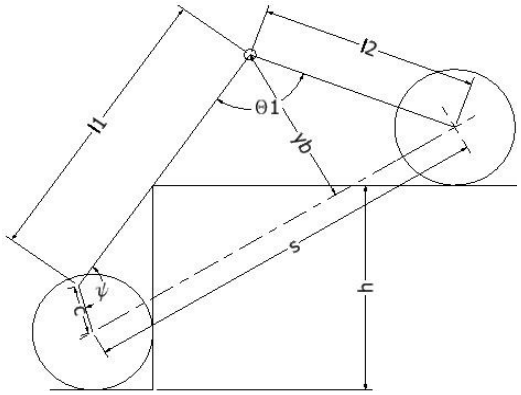

Fig. 2: Bogie intersecting the vertical step

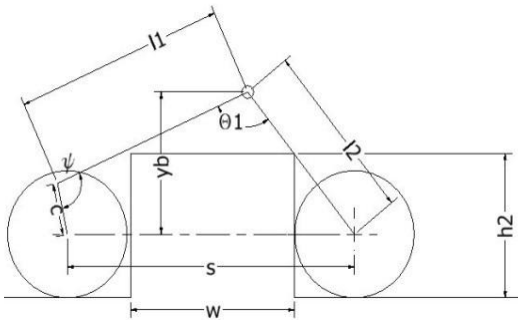

Fig. 3: Bogie intersecting the obstacle

2.2.4. Load equalization

Fig. 4 shows the external forces on single side of rocker bogie on flat ground. The force balance condition along vertical direction is given by,

$$N_1 + N_2 + N_3 = F_{cg} \tag{16}$$

Similarly the moment balance condition about the central axis of front wheel is given by,

$$N_1 \times (x_1 + x_2) + N_2 \times x_1 = F_{cg} \times x_{cg} \tag{17}$$

Since point B is a free pivot, it cannot transfer axial torque. The moment balance equation of bogie about point B is given by,

$$N_2 \times (x_b - x_1) = N_1 \times (x_1 + x_2 - x_b) \tag{18}$$

For load equalization $N_1 = N_2 = N_3$. Substituting this in above equations we obtain following relations between the design parameters,

$$x_b = x_1 + x_2/2 \tag{19}$$

$$x_{cg} = (2x_1 + x_2)/3 \tag{20}$$

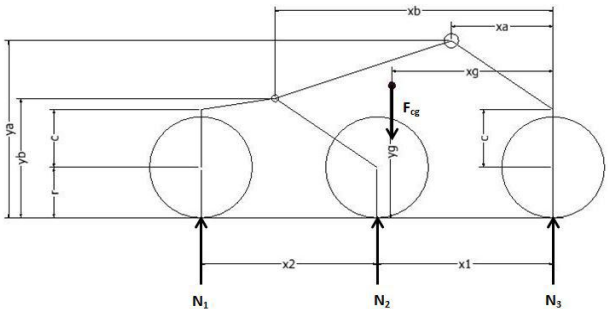

Fig. 4: Static model of single side of rocker bogie

2.3. Optimization

For simplifying the calculations, the ground profile on which rover is moving is assumed to be flat. N_w - Number of independently driven wheels, V_{rover} - Average velocity of Rover, h - Efficiency of driving motors, L_{rover} - Length of rover, W_{rover} - Weight of rover and g - Acceleration due to gravity The soil properties for calculation of driving power are based on the results for Martian soil simulants [11] and are given in Table 2.

Table 1: Optimization scenario

N_w	V_{rover}	η	L_{rover}	W_{rover}	g
6	0.01m/s	0.9	3m	900kg	3.8m/s^2

Table 2: Soil properties

Parameter	Value	Parameter	Value
γ (kg/m^3)	540	ϕ	29.48
n	0.67	N_c	27.86
k_c (kPa/m^{n-1})	67.28	N_q	16.44
k_f (kPa/m^n)	0.68	N_γ	19.34
Φ (deg)	29.48	k_{pc}	20.68
c (kPa)	1.33	k_{py}	52.61

The objective function to be minimized is defined as the weighted sum of power consumption and EGP as,

$$Objective\ Function = w_1 \times Powerconsumption / w_p + (1 - w_1) \times Groundpressure / w_{egp}$$

With constraints in Eqns. (12) – (15), (19) and (20), w_p and w_{egp} are normalizing factors which allow power consumption and EGP to be brought to a similar range. The constrained global optimization is carried out using 'Nelder Mead' method available in MATHEMATICA [12]. Fig. 5 shows the variation of objective function for different values of w_1. We assume w_1 to be 0.5, which signifies that minimizing power consumption and minimizing ground pressure are given equal importance in the design. The results of optimization are given in Table 3.

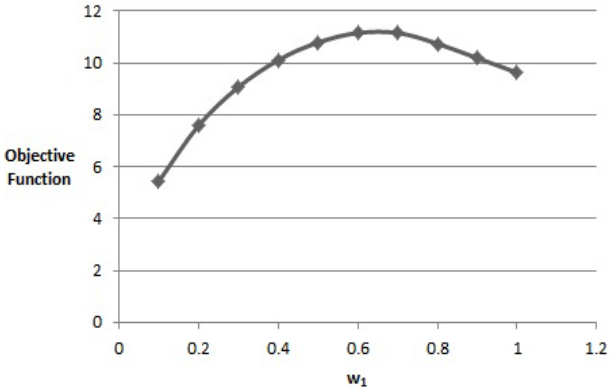

Fig. 5: Variation of objective function for different weighing factors

Table 3: Optimized design parameters

Parameter	Value	Parameter	Value
x_1	1.125	b	0.1859
x_2	1.125	x_a	$x_a < 1.2$
r	0.375	y_a	$y_a > y_b$
x_b	1.8	y_b	$y_b > 0.9$
x_g	1.2	Obj. Function	10.79

3. Wheel-soil contact model based on terramechanics approach

3.1. Slip ratio

Slips are generally observed when a rover travels on loose soil. The slip in the longitudinal direction is expressed by the slip ratio using,

$$s = \begin{cases} \dfrac{r\omega - v}{r\omega} & : |r\omega| > v \quad (accelerating) \\ \dfrac{r\omega - v}{v} & : |r\omega| < v \quad (decelerating) \end{cases} \tag{21}$$

Where v longitudinal travelling velocity of the wheel, rω circumference velocity of the wheel, r is the wheel radius and ω angular velocity of the wheel. The slip ratio assumes a value in the range from -1 to 1. When the slip ratio is -1 or 1, it indicates that the wheel has stopped moving forward/backward and is slipping in its place. When the slip ratio is zero, then it indicates a pure rolling motion.

3.2. Static wheel sinkage

When the rover is stationary, the vertical load on each wheel determines its static sinkage. According to the equation formulated by Bekker [13], the static stress p_h generated under a flat plate, which has a sinkage h and width b is calculated as follows,

$$p(h) = \left(\frac{k_c}{b} + k_{phi} \right) h^n \tag{22}$$

where k_c and k_{phi} represent pressure sinkage modules and n is the sinkage exponent. As shown in Fig. 6, for a rigid wheel over deformable terrain, the following formulae can be derived. First, the wheel sinkage h(θ) at an arbitrary angle θ is geometrically given,

$$h(\theta) = r(\cos\theta - \cos\theta_s) \tag{23}$$

where θ_s is the static contact angle. Substituting the Eqn. (23) into Eqn. (22), we obtain the variation of pressure p with θ as,

$$p(\theta) = r^n \left(\frac{k_c}{b} + k_{phi} \right) (\cos\theta - \cos\theta_s)^n \tag{24}$$

The static contact angle θ_s is numerically obtained by solving the following equation when the vertical load W is known as,

$$w = \int_{-\theta_s}^{\theta_s} p(\theta) b\, r \cos\theta d\theta = r^{n+1} \left(k_c + k_{phi} b \right) \times \int_{-\theta_s}^{\theta_s} (\cos\theta - \cos\theta_s)^n \cos\theta d\theta \tag{25}$$

Finally the static sinkage h_s is derived as follows:

$$h_s = r(1 - \cos\theta_s) \tag{26}$$

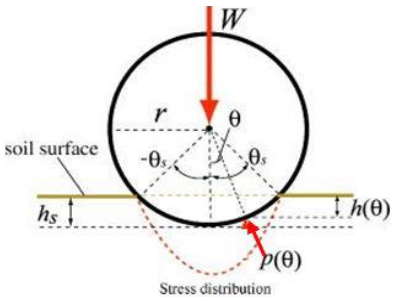

Fig. 6: Static sinkage for rigid wheel over deformable terrain [14]

3.3. Wheel contact angles and stress distribution for rotating wheel

Fig. 7 shows the model of a rotating rigid wheel on deformable terrain. The angle from the vertical to the point where the wheel initially makes contact with the soil is defined as the forward angle θ_f. Similarly the angle from the vertical to the point where the wheel departs from the soil is defined as the rear angle θ_r. The wheel contact patch on loose soil is defined by the region from θ_f to θ_r. As shown in Fig.7, the forward angle θ_f is expressed as a function of h:

$$\theta_f = \cos^{-1}\left(1 - \frac{h}{r}\right) \tag{27}$$

The rear angle θ_r is modelled by using the wheel sinkage ratio λ, which denotes the ratio between the front and the rear sinkages of the wheel as follows,

$$\theta_r = \cos^{-1}\left(1 - \frac{\lambda h}{r}\right) \tag{28}$$

$$\sigma(\theta) = \begin{cases} r^n \left(\dfrac{k_c}{b} + k_{phi} \right) \left[\cos\theta - \cos\theta_f \right]^n & : \theta_m \le \theta < \theta_f \\ r^n \left(\dfrac{k_c}{b} + k_{phi} \right) \left[\cos\left(\theta_f - \dfrac{(\theta - \theta_r)(\theta_f - \theta_m)}{\theta_m - \theta_r} \right) - \cos\theta_f \right] & : \theta_r \le \theta < \theta_m \end{cases} \tag{29}$$

The value of λ depends on the soil characteristics, wheel surface pattern and slip ratio. It decreases below 1.0 when soil compaction occurs, but can be greater than 1.0 when the soil is dug by the wheel and transported to the region behind the wheel. The value of λ is 1 when the slip ratio is zero and wheel is placed over flat terrain. The stress field below the wheel can be divided into two parts: normal stress distribution and shear stress distribution. The normal stress distribution is given by the following equation [15]. The normal stress is maximized at a specific angle θ_m given by,

$$\theta_m = (a_0 + a_1 s)\theta_f \tag{30}$$

where a_0 and a_1 are parameters that depend on the wheel-soil interaction. Their values are generally assumed as $a_0 \approx 0.4$ and $0 \leq a_1 \leq$ 0:3 [16]. The shear stress distribution $\tau(\theta)$ is given by [8],

$$\tau(\theta) = (c + \sigma(\theta)\tan\phi)\left[1 - e^{\frac{r}{k}[\theta_f - \theta] - (1-s)(\sin\theta_f - \sin\theta)}\right] \tag{31}$$

where *c* represents the cohesion stress of the soil, ϕ is the internal friction angle of the soil and *k* is the shear deformation module.

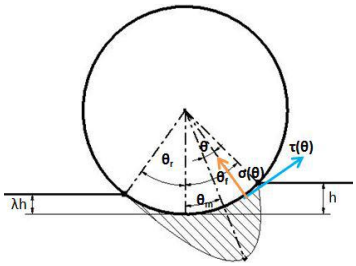

Fig. 7: Wheel contact angle and stress model

3.4. Resultant forces and torque

The normal and shear stress distributions below the wheel can be converted into resultant forces and torque acting at the wheel center. The net force in x-direction is called as the 'Drawbar Pull'. The expression for drawbar pull is obtained from the σ(θ) and τ(θ) [16] using,

$$F_x = rb\int_{\theta_r}^{\theta_f}[\tau(\theta)\cos\theta - \sigma(\theta)\sin\theta]d\theta \tag{32}$$

The net-force in y-direction is called as the 'Vertical Force' and given by Eq.32 [16]

$$F_y = rb\int_{\theta_r}^{\theta_f}[\tau(\theta)\sin\theta + \sigma(\theta)\cos\theta]d\theta \tag{33}$$

The shear stress distribution results in a net torque about the axis of rotation of the wheel passing through the wheel center which is given by,

$$T = r^2 b\int_{\theta_r}^{\theta_f}\tau(\theta)d\theta \tag{34}$$

4. Rocker bogie modelling

4.1. Simplified system model & design parameters

For simplified calculations, this work focuses on design optimization and motion dynamics of single side of the rocker bogie suspension. The analysis is valid for cases where the ground profile on either side of the rover is identical. Thus the roll and yaw motions of the chassis are neglected. Even though this assumption may not be true in natural terrain, it allows us to analyse the effect of change in design parameters on rover's performance metrics, which is the motivation behind this work. The simplified model of a single side of the rocker-bogie is shown in Fig. 8.

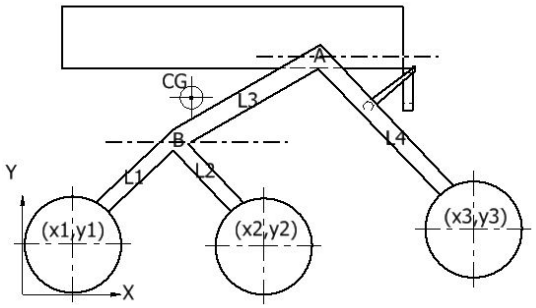

Fig. 8: 2D model of rocker bogie system

4.2. Motion dynamics

Fig. 9 shows the free body diagram (FBD) of the rover for any given configuration. F_{xi} and F_{yi} are the forces in x and y direction respectively, M_i are the moments about z-direction (out of plane), θ_{mi} are the mean contact angles. Since the rocker is connected to the bogie through a pin joint at point B, no axial torque is transmitted through the pivot B. We can consider the system to be made up of two rigid bodies: Rocker + Chassis and Bogie, connected to each other through a pin joint as shown in Fig. 10 and Fig. 11.

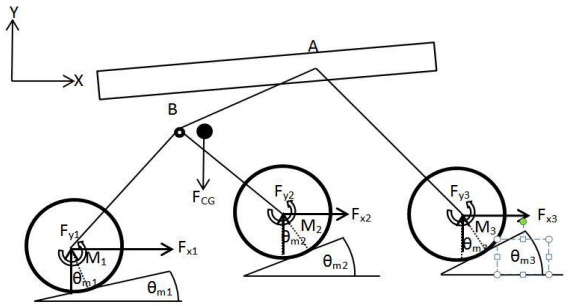

Fig. 9: Force analysis

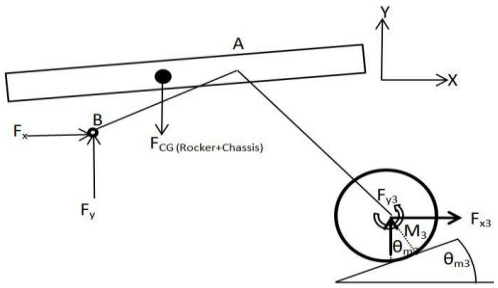

Fig. 10: Rigid body 1: Rocker + Chassis

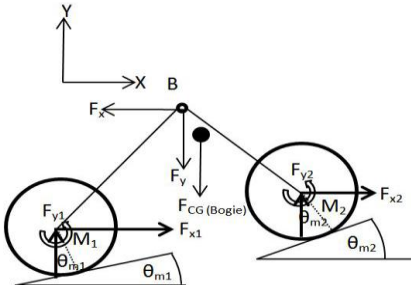

Fig. 11: Rigid body 2: Bogie

The motion of any rigid body can be defined as the combination of linear motion of its center of mass and rotation of the body about its center of mass. Thus forward dynamics equations are derived for both these rigid bodies, by considering the accelerations of center of mass and angular acceleration about center of mass as the unknown parameters. The equations for rocker+chassis as follows,

$$w_{rc} * ax_{rc} = F_x + F_{x3} \tag{35}$$

$$w_{rc} * ay_{rc} = F_y + F_{y3} - w_{rc} * g \tag{36}$$

$$I_{rc} * \alpha_{rc} = M_3 + F_{y3} * \left(x_3 - x_{cg\_rc}\right) + F_{x3} * \left(y_{cg\_rc} - y_3\right) + F_x * \left(y_{cg\_rc} - y_b\right) + F_y * \left(x_b - x_{cg\_rc}\right) \tag{37}$$

where w_{rc} - Weight of rocker and chassis, ax_{rc}, ay_{rc} - Acceleration of center of mass of rocker and chassis in x-direction and y-directions, I_{rc} - Moment of inertia of rocker and chassis about its center of mass and α_{rc} - Angular acceleration of rocker and chassis about its center of mass. The equations for bogie are as follows,

$$w_{boige} * ax_{boige} = F_x + F_{x1} + F_{x2} \tag{38}$$

$$w_{boige} * ay_{boige} = -F_y + F_{y1} + F_{y2} - w_{boige} * g \tag{39}$$

$$I_{boige} * \alpha_{boige} = M_1 + F_{y1} * \left(x_1 - x_{cg\_boige}\right) + F_{x1} * \left(y_{cg\_boige} - y_1\right) M_2 + F_{y2} * \left(x_2 - x_{cg\_boige}\right) + F_{x2} * \left(y_{cg\_boige} - y_2\right) - F_x * \left(y_{cg\_boige} - y_b\right) - F_y * \left(x_b - x_{cg\_boige}\right) \tag{40}$$

where w_{bogie} - Weight of bogie, ax_{bogie}, ay_{bogie} - Acceleration of center of mass of bogie in x-direction and y-directions, I_{bogie} - Moment of inertia of bogie about its center of mass and α_{bogie} - Angular acceleration of bogie about its center of mass.

The velocity components of any point in bogie along x and y directions can be given in terms of the velocity of its center of mass and the angular velocity about its center of mass as follows,

$$v_x = v_{x\_cgboige} + \omega_{boige} * \left(y_{cg\_boige} - y\right) \tag{41}$$

$$v_y = v_{y\_cgboige} - \omega_{boige} * \left(x_{cg\_boige} - x\right) \tag{42}$$

where x, y - Position of any arbitrary point in bogie v_x, v_y - Velocity of that arbitrary point in bogie, x_{cg_bogie}, y_{cg_bogie} - Position of center of mass of bogie, $v_{x\_cgbogie}$, $v_{y\_cgbogie}$ - Velocity of center of mass of bogie and ω_{bogie} - Angular velocity of bogie about its center of mass. Differentiating Eqns. (35) to (46) with respect to time we obtain the relation between acceleration of any point in bogie and rocket-chassis as follows,

$$a_x = a_{x\_cgboige} + \alpha_{boige} * \left(y_{cg\_boige} - y\right) + \omega_{boige} * \left(v_{y\_cgboige} - v_y\right) \tag{43}$$

$$a_y = a_{y\_cgboige} + \alpha_{boige} * \left(x_{cg\_boige} - x\right) - \omega_{boige} * \left(v_{x\_cgboige} - v_x\right) \tag{44}$$

$$a_x = a_{x\_cgrc} + \alpha_{rc} * \left(y_{cg\_rc} - y\right) + \omega_{rc} * \left(v_{y\_cgrc} - v_y\right) \tag{45}$$

$$a_y = a_{y\_cgrc} + \alpha_{rc} * \left(x_{cg\_rc} - x\right) - \omega_{rc} * \left(v_{x\_cgrc} - v_x\right) \tag{46}$$

Since the point B is common to both the bodies, we obtain following equations by Eqn. (43) with Eqn. (45) and Eqn. (44) with Eqn. (46) for $x = x_b$ & $y = y_b$ as,

$$\alpha_{boige} * \left(y_{cg\_boige} - y_b\right) + \omega_{boige} * \left(v_{y\_cgboige} - v_{y\_b}\right) + a_{x\_cgboige} = a_{x\_cgrc} + \alpha_{rc} * \left(y_{cg\_rc} - y_b\right) + \omega_{rc} * \left(v_{y\_cgrc} - v_{y\_b}\right) \tag{47}$$

$$a_{y\_cgboige} - \alpha_{boige} * \left(x_{cg\_boige} - x_b\right) - \omega_{boige} * \left(v_{x\_cgboige} - v_{x\_b}\right) = a_{y\_cgrc} - \alpha_{rc} * \left(x_{cg\_rc} - x_b\right) - \omega_{rc} * \left(v_{y\_cgrc} - v_{y\_b}\right) \tag{48}$$

So we now have 8 linear equations: Eqns. (35) to (40), Eqns. (47) and (48) with 8 unknowns viz. F_x, F_y, α_{rc}, α_{bogie}, ax_{rc}, ay_{rc}, ax_{bogie}, and ay_{bogie}. The solution of this system of equations is substituted in Eqns. (43) to (46) to get the accelerations of wheel centers, bogie pivot point B and rocker-chassis pivot point A. During the motion of rover, one or more wheels can lose contact with ground. This scenario has also been taken care of in the simulation model by substituting the wheel sinkage and resultant forces on corresponding wheels as zero in the dynamics equations.

4.3. Static load distribution

For calculating the initial sinkages of wheels, we need to obtain the initial load on each wheel when the rover is at rest. The static equilibrium equations are obtained by neglecting the acceleration, drawbar pull and resultant moment in Eqns. (35) to (40) as follows,

$$F_x = 0 \tag{49}$$

$$F_y + F_{y3} - w_{rc} * g = 0 \tag{50}$$

$$F_{y3} * \left(x_3 - x_{cg\_rc}\right) + F_y * \left(x_b - x_{cg\_rc}\right) = 0 \tag{51}$$

$$F_x = 0 \tag{52}$$

$$-F_y - w_{boige} * g = 0 \tag{53}$$

$$-F_{y1} * \left(x_1 - x_{cg\_boige}\right) - F_{y2} * \left(x_2 - x_{cg\_boige}\right) + F_y * \left(x_b - x_{cg\_boige}\right) = 0 \tag{54}$$

By solving this system of linear equations we can obtain the vertical load on each wheel i.e. F_{y1}, F_{y2}, F_{y3} in terms of the design parameters and weight data.

5. Forward dynamics simulation

The dynamic motion simulation model for the rocker bogie suspension system is implemented in MATLAB for numerical computations. Fig. 12 shows the computational flow of the motion dynamics simulation tool. For presentation of sample results, the motion dynamics simulation tool is tested using design parameters and following terrain profiles:

1. Horizontal flat ground
2. Straight incline of 20 degrees
3. Obstacle modelled by a sinusoidal profile

As shown in Fig. 13 for flat terrain the motion of wheel center and pivot points of rocker-bogie system is in

conformance with the ground profile. In this scenario, initially the rover is kept at rest and sudden torque is applied by the drive motors in the beginning. This results in initial slippage as depicted in Fig. 14.

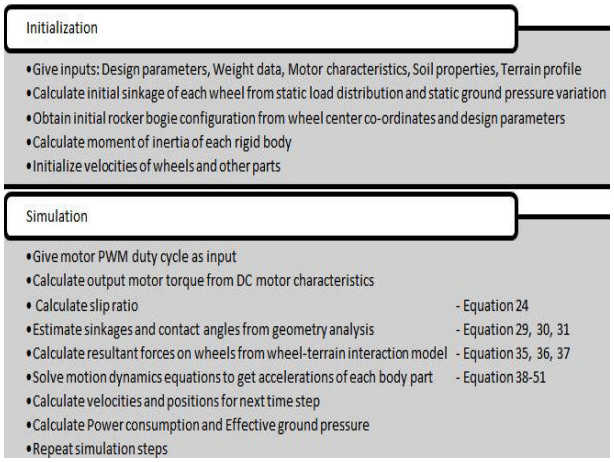

Fig. 12: Computational flow of motion dynamics simulation tool

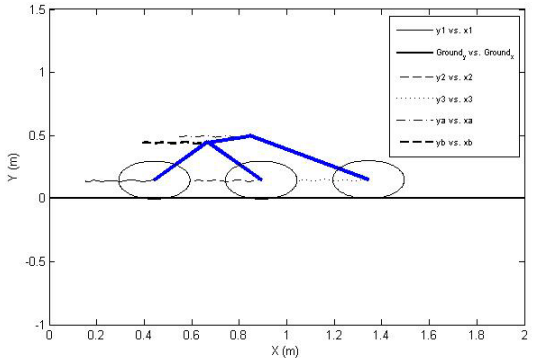

Fig. 13: Flat Terrain: Plot of ground profile and displacements of wheel centers, bogie pivot and rocker pivot

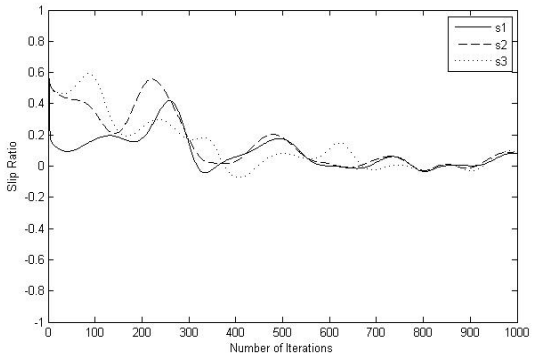

Fig. 14: Flat terrain: Plot of slip ratio vs. Number of iterations (initially rover is at rest)

The slip ratio converges to a near zero value in steady state. If the rover is initially said to be moving at a constant velocity, the slip ratio remains at a near zero value, as shown in Fig. 15. The motion of front wheel over inclination of 20 degrees is depicted in Fig. 16. In this scenario, initially the rover is assumed to travel with a constant velocity. Thus the slip ratio is initially zero, but as the front wheel starts climbing over the slope, its slip ratio increases to a magnitude of 0.2 as shown in Fig.17. The motion of rover over an obstacle of height 15cm modelled using sinusoidal ground profile is depicted in Fig. 18. In this scenario, initially the rover is assumed to travel with a constant velocity. Thus the slip ratio is initially zero, but as the front wheel starts climbing over the slope, the magnitude of its slip ratio (s_3) increases to 0.2. Later when the middle wheel starts climbing the obstacle, the slip ratios of both middle and rear wheels increase to a magnitude of about 0.2, while the slip ratio of front wheel increases further to a magnitude of about 0.3 as shown in Fig. 19.

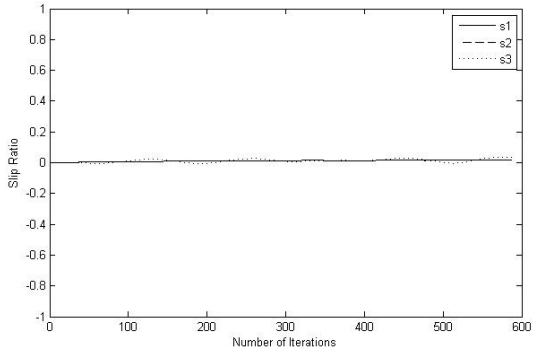

Fig. 15: Flat terrain: Plot of slip ratio vs. Number of iterations (initially rover is moving with constant velocity)

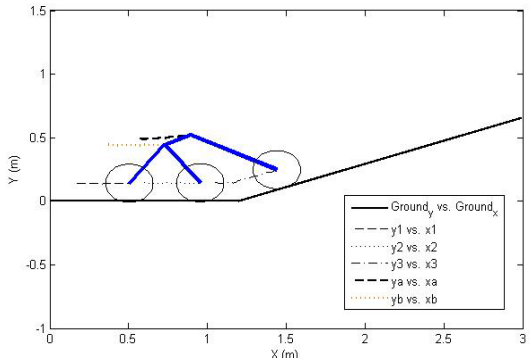

Fig. 16: Incline: Plot of ground profile and displacements of wheel centers, bogie pivot and rocker pivot

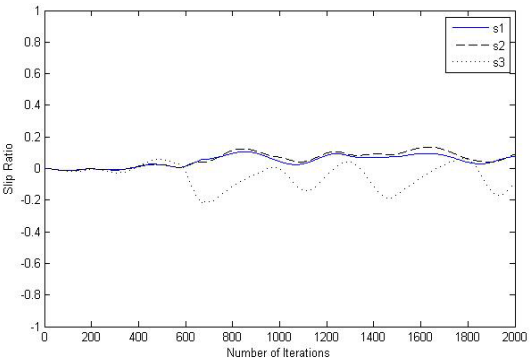

Fig. 17: Incline: Plot of slip ratio vs. Number of iterations

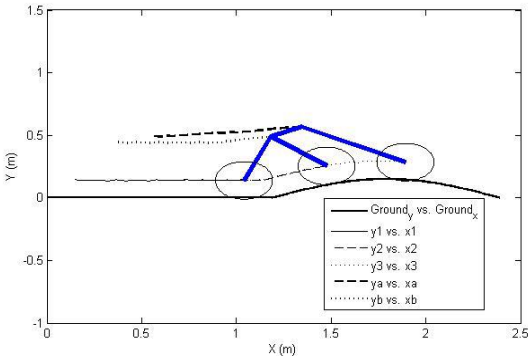

Fig. 18: Obstacle: Plot of ground profile and displacements of wheel centers, bogie pivot and rocker pivot

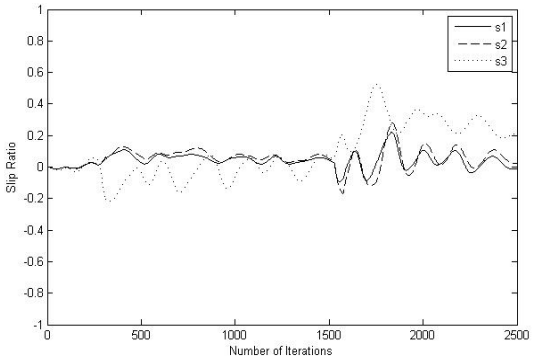

Fig. 19: Obstacle: plot of slip ratio vs. Number of iterations

6. Application of simulation tool to reconfigurable wheels

Various mechanisms have been proposed for shape changing or reconfigurable wheels. One such reconfigurable wheel prototype was developed at Massachusetts Institute of Technology [5]. In this prototype, the wheel consists of spring steel strips and wire mesh. The strips are attached to two hubcaps connected by a linear actuator. Thus when the linear actuator moves, the strips buckle and there is a change in wheel dimensions. Increase in wheel radius is accompanied by decrease in wheel width, whereas decrease in wheel radius is accompanied by increase in wheel width. A method of using a wheel with similar characteristics has been suggested in this paper. One of the major challenges in implementation of reconfigurable wheel is autonomy and control. The wheel should be able to autonomously change its shape based on the terrain characteristics on which it is moving. Some researchers have developed methods for online terrain characterization of the rover[16]. Using these techniques we can estimate the soil characteristics of the terrain on which the rover is moving. To estimate the terrain profile, vision based techniques have been proposed [17]. The terrain characteristics can be given as input to the dynamic simulation model developed in this work. By simulating the performance of rover for different wheel dimensions, we can get the optimum values of wheel dimensions for given terrain. The results of simulation can be converted into look-up tables and fed into the onboard rover software. Thus whenever a particular type of terrain is encountered the on-board controller will be able to devise the optimum wheel dimensions using these look up tables. The advantage of this method is a significant reduction in on-board computation.

For testing the effectiveness of this approach, some test scenarios have been considered in this section. The terrain characteristics for these scenarios are given in Table 4, while the soil properties for different soil types are given in Table 5. The wheel dimensions considered for this exercise are:

- Set 1: Wheel diameter = 0.13m, Wheel width = 0.22m (Min. radius)
- Set 2: Wheel diameter = 0.15m, Wheel width = 0.20m (Mean radius)
- Set 3: Wheel diameter = 0.17m, Wheel width = 0.18m (Max. radius)

For all the test scenarios and wheel dimension sets, the performance metrics: Slip ratio, power consumption and effective ground pressure are evaluated and listed in Table 6.

Table 4: Terrain characteristics for test scenarios

Test scenario	Terrain profile	Soil type
1	Upward slope of 20deg	Dry sand
2	Upward slope of 20deg	Sandy loam
3	Upward slope of 20deg	Clayey Soil
4	Sinusoidal bump of height 15cm	Dry sand
5	Sinusoidal bump of height 15cm	Sandy loam
6	Sinusoidal bump of height 15cm	Clayey soil

Table 5: Soil Parameter for various soil types [17]

	Dry Sand	Sandy Loam	Clayey Soil
n	1.1	0.7	0.5
$c(N/m^2)$	1000	1700	4140
ϕ(deg)	30	29	13
$k_c(Pa/m^{n-1})$	900	5300	13200
$k_{phi}(Pa/m^n)$	1523400	1515000	692200
k(m)	0.025	0.025	0.01

Table 6: Values of performance metrics for test scenarios

Wheel Configuration	Test scenario	Slip ratio	Effective ground pressure (N/m^2)	Power consumption (W)
Radius = 0.13m Width = 0.22m	1	0.22	3017	7.988
	2	0.5755	2806	5.256
	3	0.7936	2671	7.27
	4	0.2234	3048	8.64
	5	0.7263	2626	5.844
	6	0.8826	2758	7.814
Radius = 0.15m Width = 0.20m	1	0.1857	3001	9.797
	2	0.5514	2999	7.55
	3	0.7073	2963	8.399
	4	0.1962	2995	9.688
	5	0.629	2898	7.8
	6	0.89	3093	10.15
Radius = 0.17m Width = 0.18m	1	0.157	3096	10.608
	2	0.4541	3076	9.89
	3	0.7025	2816	11.211
	4	0.1329	3138	10.592
	5	0.6066	3017	11.587
	6	0.8588	2956	14.158

For all three performance metrics, a lower value indicates better performance. Thus for each test scenario, a 'Goodness Parameter' is assigned to each wheel configuration. The wheel configuration with lowest value of a performance metric is assigned a 'Goodness Parameter' of 100 for each test scenario. For other wheel configurations, 'Goodness Parameters' are defined as the ratio of difference between the value of performance metric for that wheel configuration and the lowest value of performance metric amongst the possible wheel configurations to the lowest value of performance metric amongst possible wheel configurations. The sum of goodness parameters for any scenario gives the 'Total Goodness Value' of each wheel configuration for given scenario. Table 7 lists the total goodness values of each

wheel configuration. Based on the 'Total Goodness Values' we can develop look-up tables for selecting the best possible wheel configuration in given scenario. Table 8 shows the look up table developed for the test scenarios considered in this section. This look up table can be used in on-board rover software to obtain the dimensions of reconfigurable wheel for best performance.

Table 7: Total goodness values for each wheel configuration in different scenarios

Test Scenario	Total goodness value		
	Wheel configuration 1	Wheel configuration 2	Wheel configuration 3
1	259	259.08	264
2	273	228.49	202
3	287	272.85	240
4	230	240.23	273
5	280	252.48	187
6	297	254.33	212

Table 8: Look up table for autonomous reconfiguration of wheel

	Upward slope	Obstacle
Dry sand	Wheel radius = 0.13m Wheel width = 0.22m	Wheel radius = 0.13m Wheel width = 0.22m
Sandy loam	Wheel radius = 0.17m Wheel width = 0.18m	Wheel radius = 0.17m Wheel width = 0.18m
Clayey soil	Wheel radius = 0.17m Wheel width = 0.18m	Wheel radius = 0.17m Wheel width = 0.18m

7. Conclusion

In this paper, the design optimization of rocker bogie mobility system and development of lookup tables for autonomous reconfigurable wheels were presented. Through a constrained optimization procedure the optimal design parameters of rocker bogie suspension system were obtained. Next, a terramechanics based motion dynamics model was developed for the rocker bogie suspension system. Wheel-ground interaction models for rigid wheel on deformable terrain was discussed. A simulation tool was developed in MATLAB, incorporating the rigid wheel over deformable terrain contact model, drive motor characteristics and motion dynamics of rocker bogie suspension system. Sample test cases were presented for the simulation tool. The concept of reconfigurable wheels was discussed with reference to the effect of wheel dimensions on performance metrics of the mobility system for different terrains. The values of three performance metrics viz. slip ratio, power consumption and effective ground pressure, were obtained using the simulation tool for some test scenarios. Based on the results for different wheel configurations, a look up table was developed for autonomous re-configuration of wheel dimensions. The method of generating such look-up tables can be extended for different soil characteristics and different kinds of operating environment.

REFERENCES:

[1] M.J. Roman. 2005. *Design and Analysis of a Four Wheeled Planetary Rover*, MSc Thesis, University of Oklahoma, USA.

[2] Resources on NASA/JPL website. http://www-robotics.jpl.nasa.gov.

[3] B.D. Harrington and C. Voorhees. 2004. The challenges of designing the rocker-bogie suspension for the mars exploration rover, *Proc. 37th Aerospace Mechanisms Symp.*, Houston, USA.

[4] T. Thuer. 2009. *Mobility Evaluation of Wheeled All Terrain Robots, Metrics and Application*, PhD Thesis, ETH Zurich.

[5] B. Bekker. 2012. *Re-inventing the Wheel for the Next Generation of Planetary Rovers*, MSc Thesis, Massachusetts Institute of Technology, USA.

[6] D. Lachat. *Antarctica Rover Design and Optimization for Limited Power Consumption*, EPFL, Switzerland.

[7] A. Petritsenko and R. Sell. 2012. Wheel motion resistance and soil thrust traction of mobile robot, *Proc 8th Int. DAAAM Baltic Conf.*, Tallin, Estonia.

[8] J.Y. Wong. 2008. *Theory of Ground Vehicles*, Wiley, New York.

[9] G.M.K. Terzaghi and R.B. Peck. 1996. *Soil Mechanics in Engg. Practice*, John Wiley and Sons.

[10] R. Lindemann. 2011. *Broader Interests and Applications the View of A JPL Hardware Engineer*, Technical Report, Jet Propulsion Laboratory, California Institute of Technology, USA.

[11] C. Brunskill, N. Patel, T.P. Gouachea, G.P. Scott, C.M. Saaj, M. Matthews and L. Cui. 2011. Characterisation of Martian soil simulants for the exomars rover test bed, *J. Terramechanics*, 48(6), 419,438.

[12] J.A. Nelder and R.A. Mead. 1965. Simplex method for function minimization, *The Computer J.*,7(4), 308-313. http://dx.doi.org/10.1093/comjnl/7.4.308.

[13] M. Bekker. 1960. *Off-The-Road Locomotion*, The University of Michigan, USA.

[14] G. Ishigami, A. Miwa, K. Nagatani and K. Yoshida. 2007. Terramechanics-based model for steering maneuver of planetary exploration rovers on loose soil, *J. Field Robotics*, 24(3), 233-250. http://dx.doi.org/10.1002/rob.20187.

[15] K. Yoshida, T. Watanabe, N. Mizuno and G. Ishigami. 2003. Terramechanics-based analysis and traction control of a lunar/planetary rover, *Proc. Int. Conf. Field and Service Robotics*, Yamanashi, Japan.

[16] J. Y. Wong and A. Reece. 1967. Prediction of rigid wheel performance based on the analysis of soil-wheel stresses - Part 1: Performance of driven rigid wheels, *J. Terramechanics*, 4(1), 81-98.

[17] K. Iagnemma, S. Kang, H. Shibly and S. Dubowsky. 2004. Online terrain parameter estimation for wheeled mobile robots with application to planetary rovers, *IEEE Trans. on Robotics*, 20(5), 921-927. http://dx.doi.org/10.1109/TRO.2004.829462.